Journal of Magnetics 17(3), 176-184 (2012) http://dx.doi.org/10.4283/JMAG.2012.17.3.176

Electrical Transport and Magnetoresistance of $La_{0.67}Ca_{0.33}MnO_3$: Ag_x (x = 0, 0.1, 0.2, 0.3, 0.4) Composites

H. Gencer*, M. Pektas, Y. Babur[1], V. S. Kolat, T. Izgi, and S. Atalay

Department of Physics, Science and Arts Faculty, Inonu University, Malatya, Turkey
[1]Department of Physics, Science and Arts Faculty, Harran University, Sanlýurfa, Turkey

(Received 3 May 2012, Received in final form 28 July 2012, Accepted 30 July 2012)

The structural, magnetic and magnetotransport properties of $La_{0.67}Ca_{0.33}MnO_3$: Ag_x (x = 0, 0.1, 0.2, 0.3 and 0.4) composites were investigated systematically. X-ray and EDX analysis indicated that Ag is not substituted into the main $La_{0.67}Ca_{0.33}MnO_3$ phase and remains an additive to the second phase at the grain boundary. The Curie temperature first decreased from 269 K for x = 0 to 257 K for x = 0.1 and then remained nearly unchanged with increasing Ag content. For the x > 0.1 samples, a second transition temperature (T_{MI2}) was observed in the resistance curves. At temperatures below 150 K, a significant enhancement in MR was observed while high temperature MR decreased with increasing Ag content. The maximum MR was observed to be 55% in the x = 0.4 sample at 10 K and a 6T magnetic field, this value is larger than that of pure $La_{0.67}Ca_{0.33}MnO_3$ (53% at 265 K and 6 T). In addition, at low fields (H < 1T), a sharp increase in the MR was observed.

Keywords : composite manganites, Ag addition, transport and magnetic properties, magnetoresistance

1. Introduction

Recently, doped perovskite manganites with the general formula $RE_{1-x}A_xMnO_3$ (RE: La, Nd, Pr; A: Ca, Sr, Pb, Ba) have attracted considerable attention due to their colossal magnetoresistance (CMR) properties. The main reason for this increasing interest in the perovskite manganites and their MR properties is because of their potential technological applications such as in magneto-resistive transducers [1], magnetic sensors [2], read or write heads in computer memory systems [3] and also in the development of spin electronic devices [4]. The physical properties of perovskite manganites have been thoroughly investigated and much effort has been expended to find the best combination of manganites with the largest MR effect. Therefore, in earlier studies, the effects of doping various elements into the manganites' A or B sites on the magnetotransport and MR properties has been extensively studied [5-12]. It was found that the MR effects of these compounds fall into two classes: intrinsic and extrinsic MR. Intrinsic MR is referred to as intragrain MR, which has a maximum near the Curie temperature and can be qualitatively explained by the Double-Exchange model [11, 12]. The extrinsic MR is referred to intergrain MR and is observed in a wide temperature range below Tc, it is attributed to spin polarized tunneling or spin-dependent scattering at the grain boundaries [13, 14].

Recently, it has been reported that the MR could be enhanced by introducing silver into the manganite matrix as a secondary phase to form ferromagnetic-metal type composites. In this context, the effect of Ag addition on the structural, magnetic, transport and MR properties in many manganite/Ag type composite systems has been investigated [15-21]. All the results have showed that the addition of Ag highly influences the grain size and nature of the grain boundary. The enhanced MR in these composite systems is thought to be due to the modification of the grain boundary effects. Therefore, silver seems to be a good candidate for an additive in manganites to enhance their MR properties. Therefore, for a better understanding of the transport mechanism and MR properties in these materials, the effect of Ag concentration on the structural, magnetic, transport and MR properties of $La_{0.67}Ca_{0.33}MnO_3$: Ag_x (x = 0, 0.1, 0.2, 0.3, 0.4) composites was investigated in detail in this work.

2. Experimental

(1-x) $La_{0.67}Ca_{0.33}MnO_3$ + xAg (x = 0, 0.1, 0.2, 0.3 and

*Corresponding author: Tel: +90 4223773743
Fax: +90 4223410037, e-mail: huseyin.gencer@inonu.edu.tr

0.4) samples were prepared in two steps. Firstly, Polycrystalline $La_{0.67}Ca_{0.33}MnO_3$ samples were prepared by a conventional solid-state reaction using high purity powder La_2O_3, $CaCO_3$ and MnO_2. The powders were mixed, grounded and pre-sintered in air at 800 °C for 12 hours. After grinding, the mixed powders were pressed into a disk shape. The disk samples were first sintered at 1200 °C for 24 h in air and after a regrinding and pelleting process final sintering was performed at 1350 °C for 24 hours in air. Secondly, Ag_2O_3 was added to the calcined LaCaMnO powder in different molar ratios. (1-x) $La_{0.67}Ca_{0.33}MnO_3$ + xAg (x = 0.1, 0.2, 0.3 and 0.4) samples were ground and pressed into pellets. Finally, all samples were heat treated at 1200 °C for 24 hours. The structural characterization was carried out using X-ray powder diffraction (Cu Ka) at room temperature. The grain structure was observed using a LEO-EVO-40 scanning electron microscope (SEM). The microstructural analysis was carried out on an energy-dispersive X-ray (EDX) system. Magnetic measurements were carried out using a Q-3398 (Cryogenic) magnetometer in a temperature range from 5 to 300 K, with a maximum magnetic field of 6 T applied. The temperature and magnetic field dependence of the resistance was measured using a Q-3398 (Cryogenic) system using the conventional four-probe method in temperatures from 5 to 300 K.

3. Results and Discussion

Fig. 1 shows the X-ray diffraction patterns of $La_{0.67}Ca_{0.33}MnO_3$: Ag_x (x = 0, 0.1, 0.2, 0.3 and 0.4) composites at room temperature. From the figure, we can see that for x = 0, a standard x-ray pattern with a cubic perovskite structure of single phase is found. Compared with the pure $La_{0.67}Ca_{0.33}MnO_3$, the x-ray patterns for the composite samples (x = 0.1, 0.2, 0.3 and 0.4) exhibit two different sets of x-ray peaks corresponding to the pure cubic perovskite structure of $La_{0.67}Ca_{0.33}MnO_3$ and the Ag phase (marked with *). Moreover, the diffraction intensity of the Ag peaks increases almost linearly with increasing Ag content and no extra phase is observed which means that there is no chemical reaction between the $La_{0.67}Ca_{0.33}MnO_3$ and Ag. The lattice constant of the undoped $La_{0.67}Ca_{0.33}MnO_3$ sample is about 3.8730, which agrees with other values in literature of 3.87 Å [22]. After Ag doping, the lattice constants were calculated to be 3.8738 Å for x = 0.1, 3.8738 Å for x = 0.2, 3.8740 Å for x = 0.3 and 3.8744 Å for x = 0.4. The lack of significant changes in lattice parameters with Ag addition shows that the Ag doping did not change the crystal structure of the $La_{0.67}Ca_{0.33}MnO_3$ phase.

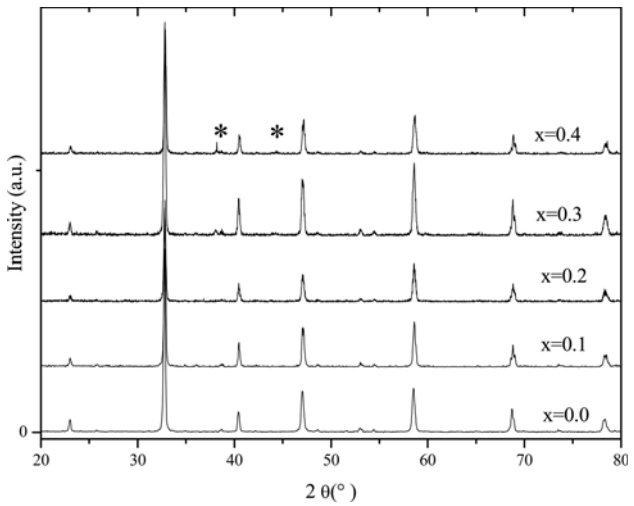

Fig. 1. X-ray diffraction patterns of $La_{0.67}Ca_{0.33}MnO_3$: Ag_x (x = 0, 0.1, 0.2, 0.3 and 0.4) composites. Asterisks indicate the metal Ag peaks.

In previous studies, many attempts have been made to substitute Ag at La-site in the manganites and also to find out the effects of Ag substitution on the structural, magnetic and conduction mechanisms [23-26]. Lakshmi *et al.* [25] reported for $La_{1-x}Ag_xMnO_3$ compounds that the samples with x < 0.2 have a single phase with a rhombohedral perovskite structure. The presence of second phase becomes apparent as Ag concentration increases gradually beyond x > 0.2. They identified the second phase as an unreacted metallic Ag phase. The existence of a second phase is thought to be due to the limited solubility of Ag in the $LaMnO_3$ main phase. The transmission electron microscopy (TEM) and electron energy loss spectroscopy (EELS) studies have also shown that Ag can not be substituted at La-sites that segregate the grain surface or grain boundary [19, 26].

Fig. 2 shows typical SEM pictures for the x = 0, 0.1, 0.3, 0.4 samples with the same magnification. It can be clearly seen from the SEM images that the all the samples show a polycrystalline nature whilst the grain size improved for the x = 0.4 sample (8-17 μm) in comparison with the x = 0 sample (1-5 μm). We used EDX analysis with the SEM to check the compositions. EDX analysis showed that while the La, Ca and Mn contents in the $La_{0.67}Ca_{0.33}MnO_3$ main phase are within the expected nominal limits, the Ag content is much lower than that of the nominal one in the $La_{0.67}Ca_{0.33}MnO_3$: Ag_x (x = 0, 0.1, 0.2, 0.3 and 0.4) composites.

There is no any clear evidence that Ag is substituted into the main $La_{0.67}Ca_{0.33}MnO_3$ phase. So one can only conclude that in the case of $La_{0.67}Ca_{0.33}MnO_3$: Ag_x, the Ag atoms remain as an additive second phase at the grain

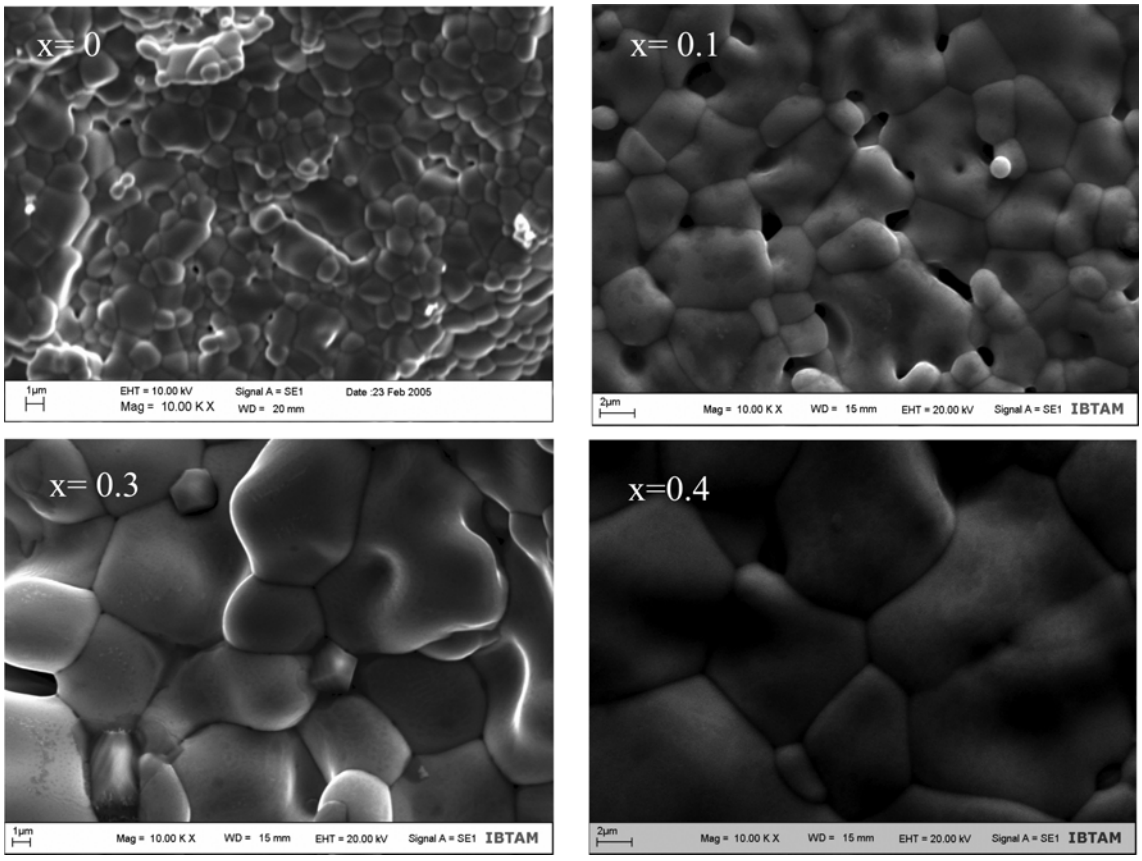

Fig. 2. SEM pictures of $La_{0.67}Ca_{0.33}MnO_3$: Ag_x for x = 0, 0.1, 0.3 and 0.4 samples with same magnification.

boundary and cause enhancement to grain size and grain connectivity. Similar behavior for grain size was observed in refs [15, 17, 18, 30]. The enhancement of grain size with Ag addition was explained by Huang *et al.* [30]. They concluded that better oxygenation of Ag helps induce better oxygenation of LCMO, this effect is attributed to the release of atomic oxygen during the decomposition of Ag_2O_3. This could be an important reason for the improvement of grain size with Ag addition.

Fig. 3(a) and (b) show the temperature dependence of magnetization for $La_{0.67}Ca_{0.33}MnO_3$: Ag_x (x = 0, 0.1, 0.2, 0.3 and 0.4) composite samples in a 0.1 T magnetic field. The plots of magnetization against the applied magnetic field (from 0 to 7 T) obtained at 240 K and 300 K are given in Fig. 3(c) for all the samples. At low temperatures, all the samples show typical ferromagnetic behavior. At a higher temperature (300 K), the M-H curves of all the samples indicate no saturation and show typical paramagnetic behavior. The saturation magnetization slightly decreases with increasing Ag content from 93 emu/g for x = 0 to 85 emu/g for x = 0.4. It is believed that the decrease in magnetization with increasing Ag content is due to the decrease in the volume fraction of the ferromagnetic $La_{0.67}Ca_{0.33}MnO_3$ phase. Additionally, the spatial distribution of doped Ag at the grain boundary and grain surface could cause extra magnetic disorder that could be another reason for the decrease in magnetization. The Curie temperature of the samples can be defined as the temperature corresponding to the peak value of the dM/dT versus T curves. We measured the Curie temperature to be at about 269 K for x = 0, 257 K for x = 0.1, 258 K for x = 0.2, 259 K for x = 0.3 and 258 K for x = 0.4 samples, in a 0.1 T magnetic field. The Curie temperature first decreases from 269 K for x = 0 to 257 K for x = 0.1 and then remains nearly unchanged with increasing Ag content. Similar behavior for the Curie temperature has been observed for $La_{0.67}Ba_{0.33}Mn_{0.88}Cr_{0.12}O_3$:$Ag_x$ [17], $La_{0.7}Ba_{0.3}MnO_3$:Ag_x [18], $La_{0.6}Sm_{0.1}Sr_{0.3}MnO_3$:CoO [27], $La_{2/3}(Ca_{0.6}Ba_{0.4})_{1/3}MnO_3$:NiO [28] and $La_{0.67}Ca_{0.33}MnO_3$:CuO [29] composites. In perovskite manganites, a considerable change in Curie temperature due to the doping concentration can be generally explained by a double-exchange interaction that is closely related to the Mn^{3+}/Mn^{4+} ratio. As evidenced by the XRD and EDX analyses, Ag is not substituted into the main $La_{0.67}Ca_{0.33}MnO_3$ phase and remains as an additive second phase at the

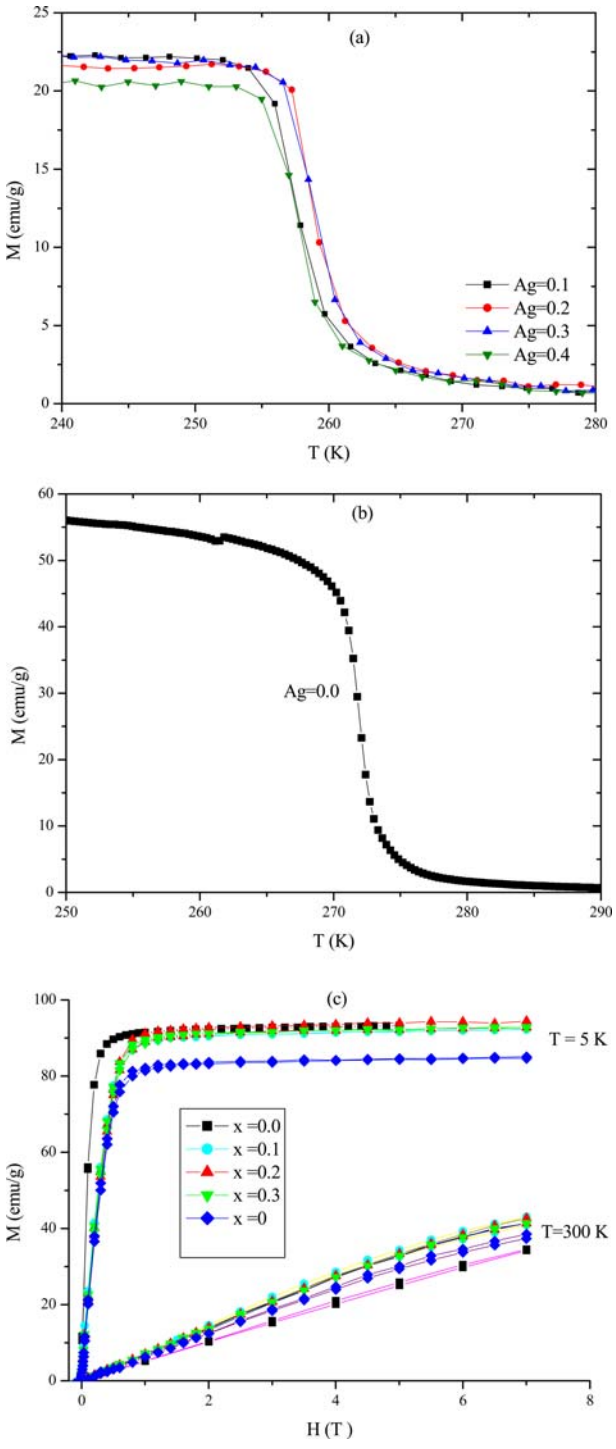

Fig. 3. (Color online) Temperature dependence of magnetization for $La_{0.67}Ca_{0.33}MnO_3$: Ag_x composite samples of (a) x = 0.1, 0.2, 0.3, 0.4, (b) x = 0 in a 0.1 T magnetic field and (c) shows the M/H curves at 5 K and 300 K.

grain boundary. In this case, the decrease in Curie temperature for x = 0.1 sample could not be explained directly by the Ag addition. The Ag addition can be considered to have an indirect effect on Curie temperature. We have not

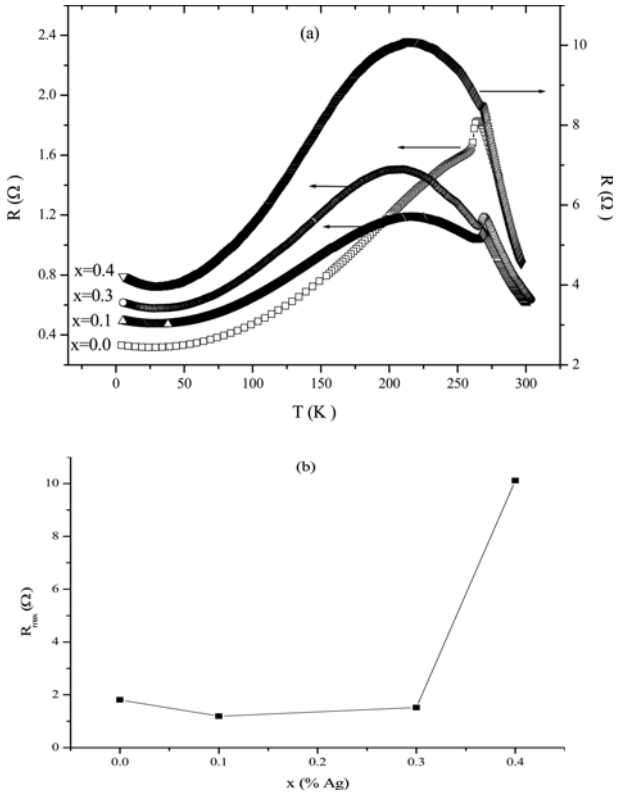

Fig. 4. (a) Temperature dependence of resistance for the $La_{0.67}Ca_{0.33}MnO_3$: Ag_x (x = 0, 0.1, 0.3 and 0.4) composite samples in a zero magnetic field. (b) The resistance vs. x curve.

performed any strain analysis, but in many reports [17, 18, 27-29] it has been concluded that the decrease in Curie temperature due to Ag addition may results from the strain, especially at grain boundaries.

Fig. 4(a) shows the temperature dependence of the resistance for the $La_{0.67}Ca_{0.33}MnO_3$: Ag_x (x = 0, 0.1, 0.3 and 0.4) composite samples at zero magnetic field in the temperature range 5-300 K.

As shown in Fig. 4(a), for undoped $La_{0.67}Ca_{0.33}MnO_3$ (x = 0) sample only one metal-insulator transition (T_{MI1}) was observed at 265 K. The value of the T_{MI1} doesn't change with increasing Ag content and is nearly identical to that of the x = 0 sample. For further addition of Ag contents a new transition temperature (T_{MI2}) was observed in the resistance curves, which is lower than T_{MI1}. It is generally known that T_{MI1} results from the intrinsic properties of manganites while T_{MI2} arises due to grain boundary effects, which are closely related to Ag concentration. It can be clearly seen from Fig. 4 that T_{MI2} first decreases from 216 K for x = 0.1 to 207 K for x = 0.3 and then again increases to 216 K for the x = 0.4 sample. Another interesting property observed in Fig. 4(b) is that the resistance value first slightly decreases from 1.84 Ω for x

= 0 to 1.18 Ω for the x = 0.1 sample and then increases to 1.51 Ω for the x = 0.3 sample. Finally the resistance jumps to a much larger value of 10.15 Ω for the x = 0.4 sample. The variation of resistance at different concentrations of Ag shows that different electrical transport properties in composites result from the effect of the dopant. The observed decrease in resistance at low Ag rates (x < 0.1) is generally attributed to the following two factors [17, 19]. Firstly, metal Ag segregated on the grain surface or grain boundaries improves the atomic structure disorder on the grain surface or grain boundaries. The barriers formed by the disordered structure of atoms on the grain surface become thinner or disappear, which leads to less electron scattering or an enhanced tunneling probability on the grain boundaries. Secondly, the existence of a good conductive metal like Ag between the grains opens a new conduction channel for electron transport. The increase in resistance for further Ag content (especially for the x = 0.4 sample) may be accounted for by the volatilization of Ag [30], which causes the emergence of lattice and structural deficiencies. These lattice and structure deficiencies create energy barriers to the electrical transport process and finally results in additional electron scattering and a sudden increase in resistance.

In order to understand the transport properties for $La_{0.67}Ca_{0.33}MnO_3$: Ag_x composite samples at low temperatures, the experimental R-T curves are fitted to the following equation:

$$\rho = \rho_0 + \rho_n T^n \quad (1)$$

where ρ_0 is the residual resistance which represents the resistance contribution due to grain boundary effects and $\rho_n T^n$ represents the higher order terms [17-19]. When n = 2 in Eq. (1), the term $\rho_2 T^2$ corresponds to the electron-electron scattering process. For n = 2.5 in Eq. (1), the term $\rho_{2.5} T^{2.5}$ represents the electron-magnon scattering process. We attempted to fit the experimental data with

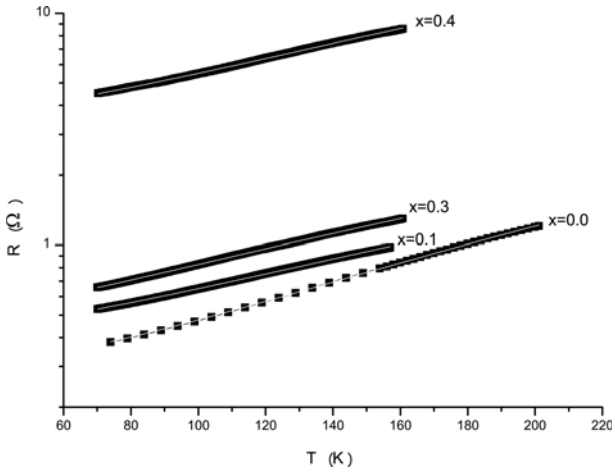

Fig. 5. Low temperature resistance curves fitted with Eq. (1). White lines indicate the good fit of experimental data.

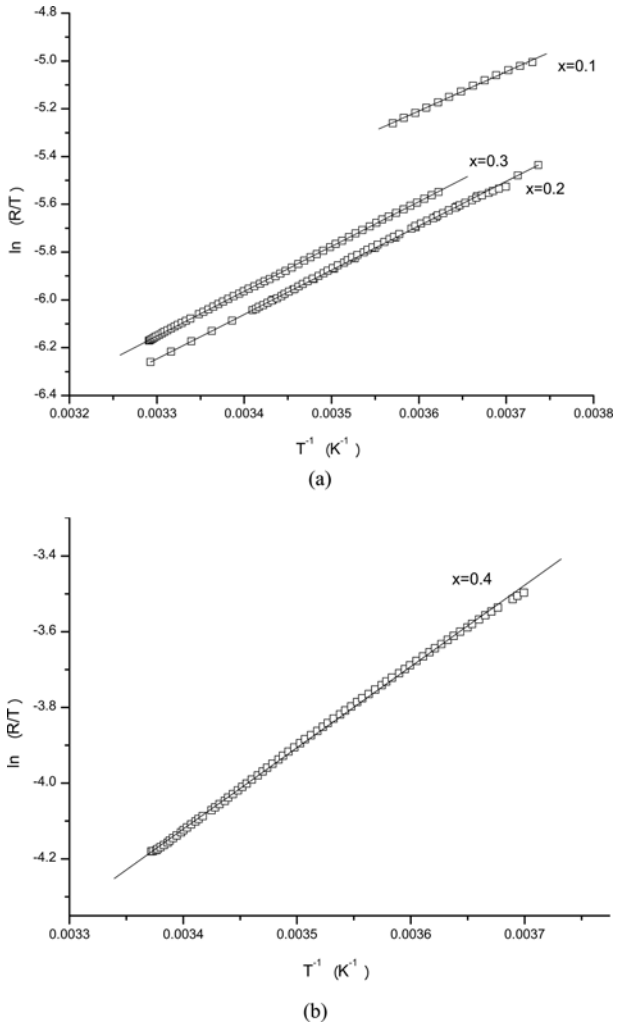

Fig. 6. Plots of ln(R/T) versus T^{-1} in the paramagnetic insulating region (a) for x = 0.1, 0.2, 0.3 and (b) for x = 0.4. Solid lines indicate a good fit of the experimental data with Eq. (2).

Table 1. Tc, T_{MI1}, T_{MI2} and transport parameters obtained from fitting the resistance data with Eq. (1) and Eq. (2).

x (%Ag)	Tc (K)	T_{MI1}(K)	T_{MI2}(K)	ρ_0 (Ω)	ρ_2 (K^{-2})	E_a (meV)
0	269	266	–	0.29046	0.46×10^{-5}	141.206
0.1	257	267	216	0.41119	3.0×10^{-5}	159.733
0.3	259	266	207	0.47001	9.0×10^{-5}	161.663
0.4	258	266	216	3.51114	20×10^{-5}	184.873

both expressions for n = 2 and n = 2.5. While the resistance data for all the samples fits well with equation $\rho_0 + \rho_2 T^2$ in (Fig. 5), which indicates the importance of the electron-electron scattering, the corresponding resistance data shows deviation from a $\rho_0 + \rho_{2.5} T^{2.5}$ dependence. The fit of experimental data to Eq. (1) shows that electron-electron scattering is the dominant process in our composite samples. The best fitting parameters (ρ_0 and ρ_2) obtained at zero magnetic field are shown in Table 1. It can be clearly seen from Table 1 that the residual resistance (ρ_0) first increases up to x = 0.1 and then stays nearly unchanged until x = 0.3. Finally ρ_0 shows a sudden increase for x = 0.4 sample. As mentioned above, ρ_0 represents the resistance contribution due to the grain boundary effect. In many studies, it has been concluded that the value of ρ_0 can be considered a measure of the effective disorder [31]. In this case the increase of ρ_0 with Ag can be interpreted as a higher value of Ag and results in poor crystallinity with a disordered grain boundary structure.

In order to understand the transport mechanism at high temperatures above Tc, the experimental R-T curves are fitted to following adiabatic small polaron hoping model,

$$\rho = \rho_0 T e^{E_a/k_B T} \quad (2)$$

where E_a is the activation energy, k_B is the Boltzmann constant and ρ_0 is the residual resistivity.

The activation energy E_a was calculated from the fitting process for a portion of the $\ln(\rho/T)$–T^{-1} curves to Eq. (2) (Fig. 6(a) and (b)). The results are given in Table 1. As can be seen from Table 1, E_a increases with Ag content. The increase in E_a with Ag content shows that the dopant was mainly distributed at the grain boundary or surface of the$La_{0.67}Ca_{0.33}MnO_3$ grains, creating energy barriers to the electrical transport process and hence giving the reason why resistance shows a considerable increase at high Ag concentration rates.

The MR of the $La_{0.67}Ca_{0.33}MnO_3$: Ag_x composite samples, defined as MR(%) = $100 \times [(R(H)-R(0))/R(0)]$, where $R(0)$ and $R(H)$ are the resistances at a magnetic field of 0 and H, respectively, were measured as a function of the magnetic field up to 6 T at various temperatures from 10 to 300 K. The results are shown in Fig. 7. The MR value reaches up to 26% in the 6 T field at 300 K for x = 0. At the same temperature, the low field MR is rather less (1.58% at 1 T). The maximum MR was seen at 265 K

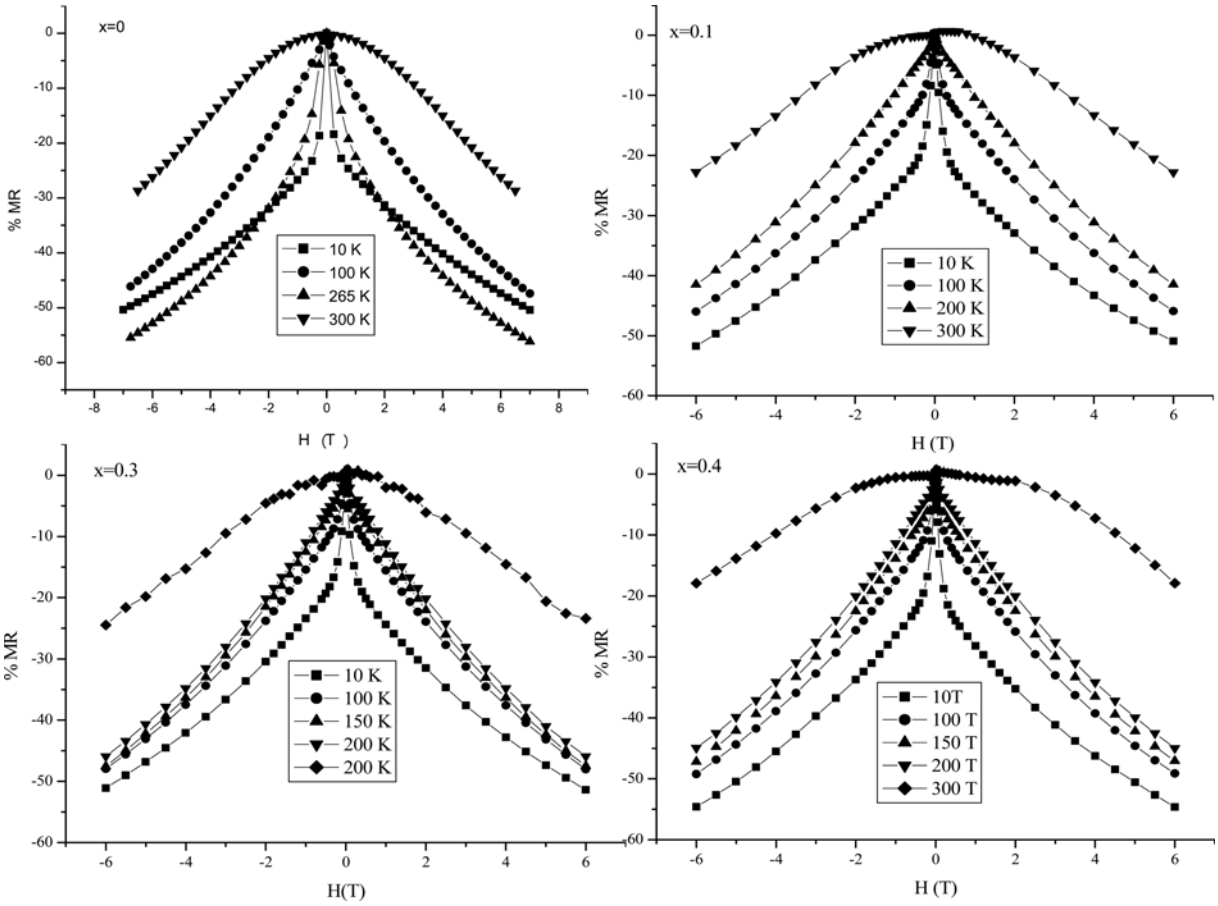

Fig. 7. MR as a function of applied field for $La_{0.67}Ca_{0.33}MnO_3$: Ag_x (x = 0, 0.1, 0.3 and 0.4) at various temperatures.

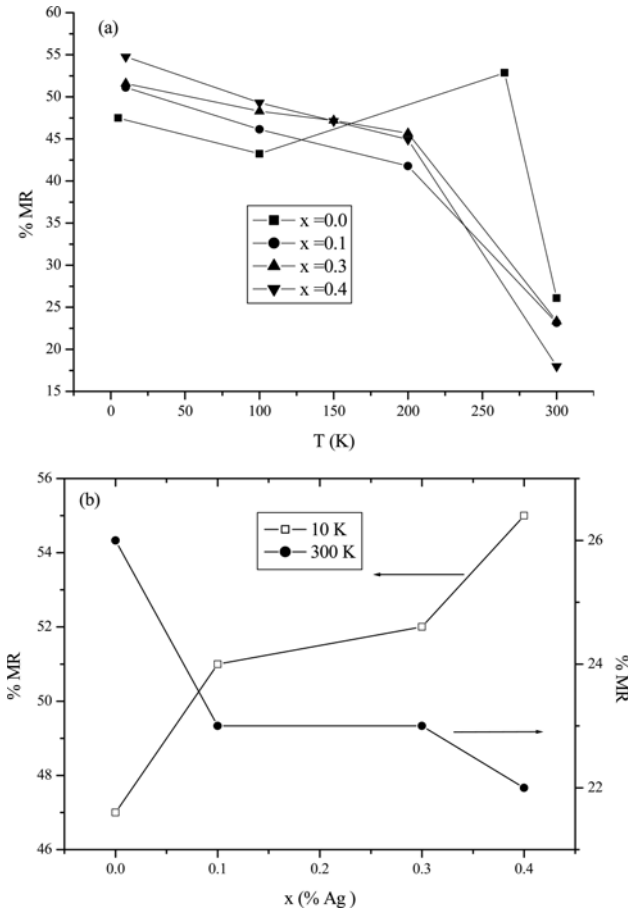

Fig. 8. (a) MR as a function of temperature at 6 T for $La_{0.67}Ca_{0.33}MnO_3$: Ag_x (x = 0, 0.1, 0.3 and 0.4). (b) MR vs. x at 10 and 300 K.

(53%). For higher Ag content samples, while the high temperature MR decreases, the low temperature MR increases. For example at 10 K in a 6 T field the maximum MR of 55% is achieved for the x = 0.4 sample.

Fig. 8(a) shows the temperature dependence of MR for the x = 0, 0.1, 0.3 and 0.4 samples at 6 T magnetic fields. As can be seen in Fig. 8(b), while the value of the low temperature MR increases, the value of the high temperature MR (near the Curie temperature) decreases with increasing Ag content. The MR value increases from 47% for x = 0 to 55% for x = 0.4 at 10 K and decreases from 26% for x = 0 to 22% for x = 0.4 at 300 K. Fig. 9 shows the magnetic field dependence of MR for the x = 0, 0.1, 0.3 and 0.4 samples at 10 and 300 K. As can be seen from Fig. 9, while the MR value at 300 K slowly increases, the MR value at 10 K increases sharply in the low field (H < 1 T) region. At a high temperature (300 K) while the x = 0.4 sample has an MR value of 18% in a 6 T magnetic field, at low temperature (10 K) the same value of MR was achieved at only 0.2 T magnetic field. In many

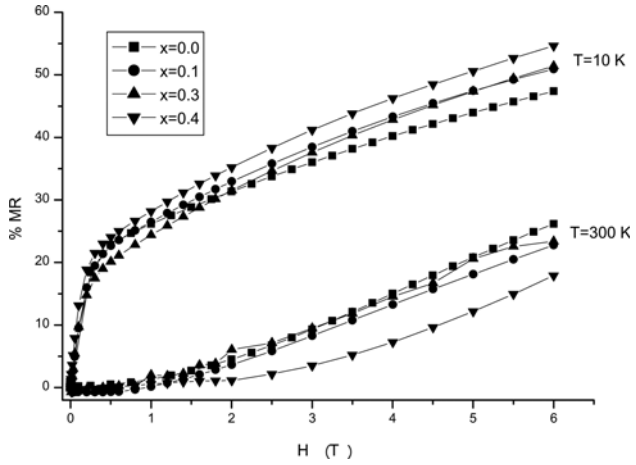

Fig. 9. MR as a function of applied field for $La_{0.67}Ca_{0.33}MnO_3$: Ag_x (x = 0, 0.1, 0.3 and 0.4) at 10 and 300 K.

studies, it has been concluded that low field MR is caused through spin disorder due to the tunneling process at the grain boundaries, when a magnetic field is applied the spin disorder is suppressed, resulting in a high MR, especially at a low field of 1 T [32]. For higher magnetic fields (H > 1 T) all the MR curves show a nearly linear increase with increasing magnetic field. Moreover, the value of the MR decreases at 300 K with increasing Ag content, whereas it increases at 10 K, which is in agreement with Fig. 8. In previous studies on composite perovskites [11, 27-34], the increase in MR values at low temperatures has been attributed to grain boundary effects introduced by the dopant. Although, the mechanism of the grain boundary induced MR is not yet clear, some models have been proposed. One of the models attributes the enhanced MR to spin-polarized tunneling through grain boundaries. Another model suggests that this behavior is due to scattering induced by spin-disorder and structure-disorder at the grain boundary. As concluded by Hwang *et al.* [34] and Gupta *et al.* [11], since the conduction electrons are almost completely polarized inside a magnetic domain, the electrons are easily transferred throughout the domain. However, when these electrons travel across grains, strong spin-dependent scattering at the boundaries leads to a high barrier. Application of a moderately low field can readily align the domains into a parallel configuration causing the resistance to drop substantially, enhancing the MR. It is generally known that the MR at high temperatures comes from intrinsic properties. The decrease of MR at high temperatures with Ag could be attributed to following two factors. Firstly, the decrease in high temperature MR could be due to the vanishing of the tunneling phenomena, which occurs only at low temperatures [32]. Secondly, for pure $La_{0.67}Ca_{0.33}MnO_3$,

the maximum MR usually appears around T_{MI} in an applied field and this is mainly responsible for the magnetic transition. With increasing x, the Ag dopant dilutes the concentration of the ferromagnetic phase of $La_{0.67}Ca_{0.33}MnO_3$ and as a consequence the intensity of the intrinsic MR decreases [33].

4. Conclusions

We systematically studied the structural, magnetic and magnetotransport properties of $La_{0.67}Ca_{0.33}MnO_3$: Ag_x (x = 0, 0.1, 0.2, 0.3 and 0.4) composites systems. X-ray, SEM and EDX analysis indicated that Ag was not substituted into the main $La_{0.67}Ca_{0.33}MnO_3$ phase and remained as an additive second phase at the grain boundary. The resistance measurements showed that there is only one metal insulator transition (T_{MI1}) for the undoped $La_{0.67}Ca_{0.33}MnO_3$ sample. For the samples with additional Ag content (x > 0.1), a second transition temperature (T_{MI2}) was observed in the resistance curves.

Interestingly, while the high temperature MR decreased (from 26% for x = 0 to 22% for x = 0.4 at 300 K), at temperatures below 150 K a significant enhancement in MR was observed with increasing Ag content under a magnetic field of 6 T. The maximum MR was observed to be 55% for the x = 0.4 sample at 10 K in a 6T magnetic field, which is larger than that the largest MR value of pure $La_{0.67}Ca_{0.33}MnO_3$ (53% at 265 K and 6T). In addition, at low fields (H < 1T), a sharp increase in MR was observed at low temperatures compared to a small increase at high temperatures. We interpret the enhanced low field MR at low temperatures to be related to spin polarized tunneling across the grain boundaries.

Acknowledgements

This work was supported by Inonu University research fund with the project number 2011/29.

References

[1] A. P. Nosov, V. G. Vasilev, E. V. Vladimirova, E. V. Mikhaleva, B. V. Slobodin, and V. V. Ustinov, Russian J. Nondestructive Testing **37**, 181 (2001).
[2] L. Balcells, E. Calvo, and J. Fontcuberta, J. Magn. Magn. Mater. **242**, 1166 (2002).
[3] A. P. Ramirez, J. Phys.: Condens. Matter. **9**, 8171 (1997).
[4] M. Kawasaki, M. Izumi, Y. Konishi, T. Manako, and Y. Tokura, Mater. Sci. Eng. B **63**, 49 (1999).
[5] V. S. Kolat, H. Gencer, and S. Atalay, Physica B **371**, 199 (2006).
[6] C. N. R. Rao and A. K. Cheetham, Science **272**, 369 (1996).
[7] V. S. Kolat, H. Gencer, M. Gunes, and S. Atalay, Mater. Sci. Eng. B **140**, 212 (2007).
[8] M. H. Phan and S. C. Yu, J. Magn. Magn. Mater. **308**, 325 (2007).
[9] V. S. Kolat, T. İzgi, A. O. Kaya, H. Gencer, N. Bayri, and S. Atalay, J. Magn. Magn. Mater. **322**, 427 (2010).
[10] H. Gencer, V. S. Kolat, and S. Atalay, J. Alloy. Compd. **422**, 40 (2006).
[11] A. Gupta, G. Q. Gong, G. Xiao, P. R. Duncombe, P. Lecoeur, P. Trouilloud, Y. Y. Wang, V. P. Dravid, and J. Z. Sun, Phys. Rev. B **54**, R15629 (1996).
[12] M. Gunes, H. Gencer, V. S. Kolat, S. Vural, H. I. Mutlu, and S. Atalay, Mater. Sci. Eng. B **136**, 41 (2007).
[13] J. M. D. Coey, J. Appl. Phys. **85**, 5576 (1999).
[14] T. Zhu, B. G. Shen, J. R. Sun, H. W. Zhao, and W. S. Zhan, Appl. Phys. Lett. **78**, 3863 (2001).
[15] V. P. S. Awana, R. Tripathi, S. Balamurugan, H. Kishan, and E. T. Muromachi, Solid State Commun. **140**, 410 (2006).
[16] S. Pal, A. Banerjee, S. Chatterjee, A. K. Nigam, B. K. Chaudhuri, and H. D. Yang, J. Appl. Phys. **94**, 3485 (2003).
[17] X. B. Yuan, Y. H. Liu, N. Yin, C. J. Wang, and L. M. Mei, J. Magn. Magn. Mater. **306**, 167 (2006).
[18] R. Tripathi, V. P. S. Awana, H. Kishan, S. Balamurugan, and G. L. Bhalla, J. Supercond. Nov. Magn. **21**, 151 (2008).
[19] N. Panwar, D. K. Pandya, and S. K. Agarwal, J. Phys.: Condens. Matter. **19**, 456224 (2007).
[20] R. Tripathi, V. P. S. Awan, N. Panwar, G. L. Bhalla, H. U. Habermier, S. K. Agarwal, and H. Kishan, J. Phys. D: Appl. Phys. **42**, 175002 (2009).
[21] R Tripathia, V. P. S. Awana, H. Kishana, and G. L. Bhalla, J. Magn. Magn. Mater. **320**, L89 (2008).
[22] X. X. Zhang, J. Tejeda, Y. Xin, G. F. Sun, K. W. Wong, and X. Bohigas, Appl. Phys. Lett. **69**, 3596 (1996).
[23] L. Pi, M. Hervieu, A. Maignan, C. Martin, and B. Raveau, Solid State Commun. **126**, 229 (2003).
[24] M. Battabyal and T. K. Dey, J. Phys. Chem. Solids **65**, 1895 (2004).
[25] Y. K. Lakshmi and P. V. Reddy, J. Magn. Magn. Mater. **321**, 1240 (2009).
[26] Q. Y. Xu, R. P. Wang, Z. Zhang, Phys. Rev. B **71**, 092401 (2005).
[27] C. Shuiyuan, Y. Qingying, L. Heng, H. Shangbo, and H. Zhigao, J. Rare Earths **24**, 788 (2006).
[28] S. Chen, H. Lai, Y. Lin, W. Ke, F. Zheng, Z. Huang, and Y. Du, J. Magn. Magn. Mater. **303**, e308 (2006).
[29] J. H. Miao, S. L. Yuan, X. Xiao, G. M. Ren, G. Q. Yu, Y. Q. Wang, and S. Y. Yin, J. Appl. Phys. **101**, 043904 (2007).
[30] Y. H. Huang, K. F. Huang, F. Luo, L. L. He, Z. M. Wang, C. S. Liao, and C. H. Yana, J. Solid State Chem. **174**, 257 (2003).

[31] S. Mercone, C. A. Perroni, V. Cataudella, C. Adamo, M. Angeloni, C. Aruta, G. De Filippis, F. Miletto, A. Oropallo, P. Perna, A. Yu. Petrov, U. S. Uccio, and L. Maritato, Phys. Rev. B **71**, 064415 (2005).

[32] A. Gaur and G. D. Varma, J. Alloy. Compd. **453**, 423 (2008).

[33] Y. H. Xiong, X. C. Bao, J. Zhang, C. L. Sun, W. H. Huang, X. S. Li, Q. J. Ji, X. W. Cheng, Z. H. Peng, N. Lin, Y. Zeng, Y. F. Cui, and C. S. Xiong, Physica B **398**, 102 (2007).

[34] H. Y. Hwang, S. W. Cheong, N. P. Ong, and B. Batlogg, Phys. Rev. Lett. **77**, 2041 (1996).